Estimation of Three-Phase Flow Functions in Porous Media

G. M. Mejia, A. T. Watson, and J. E. Nordtvedt
Dept. of Chemical Engineering, Texas A&M University, College Station, TX 77843

Several important processes involve the flow of three immiscible fluids through porous media, such as the flow of oil, water and gas in petroleum reservoirs, or water, non-aqueous-phase liquid and air in underground aquifers. Multiphase flow functions (relative permeability and capillary pressure) are important to simulate the flow in such systems. Unfortunately, there are few, if any, reliable estimates of these flow properties from laboratory experiments. One of the main reasons for this is the use of unsupported simplifications in the procedures for determining property estimates from measured data.

We present a method for simultaneous estimation of three-phase relative permeability and capillary pressure functions from laboratory experiments. The method is not limited by restrictions in the experimental design or assumptions regarding the saturation dependence or shape of the functions to be estimated. The method is demonstrated with simulated experiments. It is shown that with a suitable experimental design, regions of the functions represented by the measured data can be determined accurately.

Introduction

The mathematical modeling and simulation of the flow of fluids through porous media is an essential planning exercise for many industrial processes, including the production of fluids from petroleum reservoirs and remediation of underground water resources. The mathematical models are typically based on continuum representations in which state variables are defined relative to representative volume elements, or local volume averages (Bear, 1972; Slattery, 1981). There are several porous media properties that must be determined in order to simulate fluid flow. In situations for which there are multiple fluid phases, relative permeability and capillary pressure functions are required. These are functions of fluid saturation; we refer to them here as *multiphase flow functions*.

It is important to be able to determine these functions from laboratory experiments on porous medium samples. For applications concerned with underground reservoirs or aquifers, it may be desirable to estimate these functions on the basis of flow data measured at wells (Watson et al., 1980); even so, it is important to incorporate into the estimation process properties determined in the laboratory from representative samples (Yang and Watson, 1991). Laboratory experiments may also be used in studies directed to the determination of effects of various operating scenarios on the properties, such as additives to injection fluids.

The relative permeability functions are defined through an extension of Darcy's law to each fluid phase, namely $v_i = -(kk_{ri}/\mu_i)\partial P_i/\partial z$. This linear relationship between the superficial velocity and the pressure gradient is adequate for describing capillary dominated flow, that is, flow for which the capillary number ($N_{\text{cap},i} = \mu_i v_i/\sigma$) is relatively small (see, e.g., Dullien, 1992). Under these conditions, the relative permeability is independent of the capillary number, depending only on fluid saturation and its history. Otherwise, the relative permeability may depend upon the fluid velocity, and possibly other quantities. As reservoir flow is generally capillary dominated, laboratory experiments should be conducted under corresponding conditions.

Relative permeabilities cannot be measured directly. Instead, displacement experiments can be conducted in which various quantities are measured, such as pressure drop and fluid production, and estimates of the relative permeabilities determined by calculation from an appropriate mathematical model of the experiment. This calculational procedure is referred to as the inverse problem. This inverse problem is particularly challenging since the properties to be estimated are *functions* that appear in partial differential equation models.

Correspondence concerning this article should be addressed to A. T. Watson.
Present addresses of: G. M. Mejia, ITESM, Monterrey, N.L., Mexico; J. E. Nordtvedt, RF-Rogaland Research, Thormøhlensgt. 55, N-5008 Bergen, Norway.

A simplification of the inverse problem can be obtained if capillary pressure is neglected. Then, the displacement experiment can be represented by a set of partial differential equations that can be solved analytically. This solution forms the basis for a commonly used method in which relative permeability values corresponding to discrete values of saturation are explicitly calculated based on that analytical solution (Johnson et al., 1958). This approach has several numerical problems: it requires calculation of derivatives of data, which can lead to substantial estimation errors (Tao and Watson, 1984), and it provides estimates of the relative permeability at only a discrete set of saturation values (Richmond and Watson, 1990). Furthermore, the effects of capillary pressure can cause significant estimation errors (Richmond, 1988). Capillary effects are persistent in these types of experiments, and elimination of those effects would likely require experimental conditions well outside of the capillary-dominated regime. It is preferable to account for capillary pressure effects in solving the inverse problem. In principle, this can be done by determining the capillary pressure function on the sample of interest through an independent experiment (see, e.g., Hassler and Brunner, 1945; Nordtvedt and Kolltveit, 1991), and including the capillary pressure within the mathematical model of the experiment. However, there are a number of difficulties in running sequential experiments on a single sample, including reestablishing wetting conditions and initial saturation states and ranges. Also, the experimental time can be inordinately long. The use of properties determined from a companion sample would lead to estimation errors of unknown magnitude. It is much more desirable to determine the capillary pressure and relative permeability functions simultaneously from a single experiment.

A method has been developed for estimating relative permeability and capillary pressure functions simultaneously from experiments (Watson et al., 1988). The unknown functions are adjusted within a mathematical model of the experiment so that the simulated data "match" the data measured in the experiment. All the appropriate physical effects can be incorporated into the mathematical model of the experiment. The utility of the method has been demonstrated by analyzing dynamic displacement experiments (both conventional pressure drop and production data (Richmond and Watson, 1990) as well as with *in situ* saturation measurements (Mejia et al., 1994)), centrifuge displacement experiments (Nordtvedt et al., 1993), and steady-state-type displacement experiments (Nordtvedt et al., 1994).

To date, no method for estimating three-phase flow functions has been presented. All the work directed to three-phase relative permeabilities has been directed toward *pointwise* calculation of those properties, and the estimation of three-phase capillary pressure has hardly been addressed. Two approaches have been explored for calculating three-phase relative permeability values. In the first approach, three-phase relative permeabilities are *predicted* from two-phase relative permeabilities using hypothesized models (see Baker, 1988, for an overview of such models). The second approach is to calculate them from production and pressure drop data gathered during displacement experiments on laboratory samples.

The two most commonly used models for predicting three-phase relative permeability from two-phase relative permeability were developed by Stone (1970, 1973). Both of these models use the assumption that each relative permeability is a function of its own saturation, except for the intermediate-wetting phase permeability, which is a function of two saturation. Variations of Stone's models (Dietrich and Bondor, 1976; Fayers, 1989) and other models (e.g., Aleman and Slattery, 1988; Robinson and Slattery, 1994) have been proposed. Reliable methods for predicting three-phase relative permeability are clearly desirable since one could avoid the corresponding three-phase experimentation. However, it is essential that these models be evaluated with actual experimental data; sufficient laboratory measurements of three-phase flow functions for this purpose are not currently available.

Three-phase relative permeability values have been calculated pointwise from steady-state displacement experiments (Leverett and Lewis, 1941; Caudle et al., 1951; Corey et al., 1956; Saraf and Fatt, 1967; Schneider and Owens, 1970; Dria et al., 1990; Oak, 1990; Oak et al., 1990; Oak and Ehrlich, 1988). In the steady-state experiment, two or three fluids are injected into the core sample with constant flow rates until the pressure drop no longer changes. At this point, it is assumed that steady-state has been achieved, and fluid productions (or saturation profiles) and pressure drop are measured. Then the flow rates are changed and the displacement continues until another steady-state is achieved. This procedure is repeated several times to generate average saturations (which are computed from material balances if fluid productions are measured) and pressure-drop values corresponding to one displacement experiment. If one assumes that the saturation is uniform at each steady-state, relative permeability values corresponding to each average saturation value can be calculated directly from Darcy's law. The time required to perform these experiments can be extraordinarily long, so relatively few relative permeability values can ever be expected. Reliable estimation of the entire functions from such few values is very unlikely. Indeed, it is generally not attempted. Also, the neglect of capillary pressure can lead to significant errors in the calculated values.

Dynamic displacement experiments have also been used for estimating three-phase relative permeability. In those experiments, a sample is initially saturated with one or two fluids, and one or two fluids are injected. Production and pressure drop data are collected. These experiments can be completed within several hours, offering a substantial advantage compared to the steady-state experiments (Saraf et al., 1982; Spronsen, 1982; Sarem, 1966). Relative permeability values are calculated using an explicit method (Sarem, 1966) that is an extension of the method of Johnson et al. (1958). The method is based on the assumption that the fractional flow of each fluid phase is a function of its own saturation alone. This assumption has not been supported experimentally; several studies with steady-state experiments (see Manjnath and Honarpour, 1984, for an overview) indicate the relative permeabilities are generally functions of two saturations. Some variations of the Sarem method have appeared (Grader and O'Meara, 1988; Spronsen, 1982); in particular, Virnosky (1985) overcomes that assumption. However, none of the studies overcomes the problems associated with computing derivatives of measured data, obtaining estimates of the entire functions, or avoiding estimation errors that will result from the neglect of capillary pressure effects in the analysis.

In sum, the determination of reliable estimates of three-

phase relative permeability functions from experimental data is a problem that is largely unworked. Previous studies have ignored capillary pressure, even though those effects will likely be significant in experiments run at conditions comparable to those encountered in reservoir flows. Furthermore, those methods have not provided estimates for the entire functions.

In this article, we present a method for simultaneous estimation of three-phase relative permeability and capillary pressure functions from experimental data. The method is quite general: there are no specific limitations regarding experimental conditions, and no assumptions are made regarding the dependency of the multiphase flow functions on saturation. We also provide measures of the accuracy of the estimates and show that when sufficient experimental data are available, accurate estimates of these functions can be obtained. A number of challenges do remain. In particular, we have not yet demonstrated the method with actual experimental data. Due to the great investment required to run three-phase relative permeability experiments, we intend to study various options and merits of different experimental designs prior to conduct of the experiments. This reported study provides the required computational tools for such a study of the experimental design.

Methodology

The process used for estimating three-phase multiphase flow functions has evolved from a regression-based method originally presented for estimating two-phase flow functions (Watson et al., 1988). There are several principal elements. A mathematical model is selected to represent the displacement experiment. The model should be sufficiently complete so that all the important physical effects within the experiment are represented by that model. Functional representations are to be chosen for the multiphase flow functions that are to be estimated; since ultimately a finite set of data are collected, our unknown functions must be represented with a finite number of parameters. The estimation of the properties can then be posed as a parameter estimation problem, in which the coefficients within the functional representations are calculated as those that minimize a suitable objective function.

In this section, the mathematical model and estimation procedure used are described. The method used to analyze the accuracy with which the properties can be estimated from measured data is also described.

Mathematical model

The mathematical model comprises a Darcy equation and continuity equation for each fluid phase (Aziz and Settari, 1979):

$$\nabla\cdot\left[\frac{kk_{ri}}{\hat{V}_i\mu_i}\left(\nabla P_i-\rho_i\frac{g}{g_c}\nabla z\right)\right]=\frac{\partial(\phi S_i/\hat{V}_i)}{\partial t}+q_i \quad i=1,2,3 \quad (1)$$

$$P_{c21}=P_2-P_1 \quad (2)$$

$$P_{c32}=P_3-P_2 \quad (3)$$

$$S_1+S_2+S_3=1. \quad (4)$$

The subscripts 1, 2 and 3 refer to each of the three immiscible fluid phases. Several finite difference methods have been proposed to solve this set of coupled, nonlinear partial differential equations. We solved the system implicitly using a variation of the simultaneous-solution method (Aziz and Settari, 1979). The solution of the model and the boundary conditions used are discussed by Velazquez (1992).

These equations are quite general, including the effects of compressibility and allowing for spatial variations of the porosity and permeability and even zonal variations of the multiphase flow functions. Mejia et al. (1994) have considered the estimation of two-phase flow functions where spatial variation of porous media properties were considered. For simplicity in this study, we have taken all the porous media properties to be uniform.

Functional representations

In general for three-phase situations, there are three relative permeability functions (one for each phase) and two capillary pressure functions (one for each of two fluid pairs; the function corresponding to the third fluid pair is not independent) to be estimated. Each of these functions will, in general, depend on two saturations (the third saturation is not independent). Each function represents a surface on a plot with two saturations. This situation represents additional complexities compared to two-phase systems. In those cases, three functions are to be estimated (two relative permeability and one capillary pressure). Each function depends on only one variable (the saturation), so that they can be plotted as curves.

The unknown functions to be estimated must be represented with a finite number of parameters. This is accomplished through selection of functional representations for the properties to be estimated. It is very important that the selected functional representations be capable of accurately representing the *true* (but unknown) functions (Kerig and Watson, 1986). This is accomplished very well for the two-phase case through the use of B-splines, since they can represent any smooth function arbitrarily accurately. At the same time, B-splines have a number of desirable computational features (Schumaker, 1981). For the two-phase case, the relative permeability and capillary pressure functions can be written as

$$k_{ri}(S_1)=\sum_{j=1}^{M_{ri}^1+K_{ri}^1} a_j^i B_j^{M_{ri}^1}(S_1,\mathbf{y}^{ri}) \qquad i=1,2 \quad (5)$$

$$P_c(S_1)=\sum_{j=1}^{M_{c21}^1+K_{c21}^1} c_j^{21} B_j^{M_{c21}}(S_1,\mathbf{y}^{c21}), \quad (6)$$

where M_{ri}^1 and K_{ri}^1 are the spline order and the number of knots (simple knots assumed), respectively, for the relative permeability. Similarly, M_{c21}^1 and K_{c21}^1 are the spline order and the number of knots, respectively, for the capillary pressure. The functions $B_j^{M_i^1}(S_1,\ \mathbf{y}^i)$ are the B-spline basis functions, uniquely determined by the spline order (M_i^1) and the extended partition vector, $\mathbf{y}^i$ ($i=r1$, $r2$, or $c21$). Further details on B-splines may be found elsewhere (Schumaker, 1981; de Boor, 1978).

We have extended this approach to the three-phase case by using bivariate splines for representing the flow functions. In particular, we have used tensor-product B-splines (Schumaker, 1981), which are given by

$$k_{ri}(S_I,S_{II}) = \sum_{k=1}^{M_{ri}^I + K_{ri}^I} \sum_{l=1}^{M_{ri}^{II} + K_{ri}^{II}} a_{k,l}^i B_{k,l}(S_I,S_{II},y^I,y^{II}) \qquad i=1,2,3 \quad (7)$$

$$P_{cij}(S_I,S_{II}) = \sum_{k=1}^{M_{cij}^I + K_{cij}^I} \sum_{l=1}^{M_{cij}^{II} + K_{cij}^{II}} c_{k,l}^{ij} B_{k,l}(S_I,S_{II},y^I,y^{II}) \qquad ij=21 \text{ or } 32, \quad (8)$$

where M_{ri}^k and K_{ri}^k are the spline order and the number of knots for the relative permeabilities of phase i in the S_k direction, respectively. The corresponding quantities for the capillary pressure between phases i and j are M_{cij}^k and K_{cij}^k. Directions I and II can be along any two saturation axes.

It should be noted that few studies have ever considered candidate functional representations for three-phase flow functions. One study has proposed a power-model representation that was tested by estimating parameters to fit relative permeability points (Parmeswar and Maerefat, 1986). Given the lack of success of these types of models in two-phase cases (see discussion in Kerig and Watson, 1987), their utility for this situation is doubtful.

Estimation procedure

The determination of the coefficients within the B-spline representations are carried out by solving a minimization problem (Watson et al., 1988; Kerig and Watson, 1986). An objective function is formulated as a weighted sum of squared differences between the measured data and corresponding values calculated from the mathematical model of the experiment:

$$J(\boldsymbol{\beta}) = [\boldsymbol{Y} - \boldsymbol{F}(\boldsymbol{\beta})]^T \boldsymbol{W} [\boldsymbol{Y} - \boldsymbol{F}(\boldsymbol{\beta})] \quad (9)$$

where $\boldsymbol{Y}$ is a vector of data measured in the experiment and $\boldsymbol{F}(\boldsymbol{\beta})$ are the corresponding values calculated with the mathematical model of the experiment. The vector $\boldsymbol{\beta}$ is composed of the coefficients within the B-splines, which is

$$\boldsymbol{\beta} = \left[a_1^1,\ldots,a_{N_{r1}}^1, a_1^2,\ldots,a_{N_{r2}}^2, a_1^3,\ldots,a_{N_{r3}}^3, c_1^{21},\ldots,c_{N_{c21}}^{21}, c_1^{32},\ldots,c_{N_{c23}}^{32} \right]^T. \quad (10)$$

Here, the a_i^j are the coefficients in the representation of the relative permeability for phase j, and the c_i^{21} and c_i^{32} are the coefficients for the capillary pressure between phases 2–1 and 3–2, respectively. Note that $N_{ri} = (M_{ri}^I + K_{ri}^I)(M_{ri}^{II} + K_{ri}^{II})$ for $i = 1,2,3$, and $N_{cij} = (M_{cij}^I + K_{cij}^I)(M_{cij}^{II} + K_{cij}^{II})$ for $ij = 21$ and 32. The weighting matrix $\boldsymbol{W}$ is selected according to statistical criteria so that, with appropriate choices of the mathematical model and extended partition, maximum-likelihood estimates are obtained (Bard, 1974). Generally, it can be taken to be a diagonal matrix with entries equal to the inverse of the estimated variances of the data measurement errors (Weisberg, 1985).

The minimization procedure can be speeded and made more robust by including constraints on the estimated parameters. For example, each of the functions is taken to be monotonic with saturation, and the relative permeability functions are taken to be nonnegative. These can be implemented as linear inequality constraints (Watson et al., 1988; Richmond and Watson, 1990; Richmond, 1988):

$$\boldsymbol{G\beta} \geq \boldsymbol{g}. \quad (11)$$

The determination of the value of $\boldsymbol{\beta}$ that minimizes Eq. 9 was obtained with a trust region implementation of the Levenberg–Marquardt algorithm that incorporates the linear inequality constraints (Watson et al., 1988).

Several different procedures have been reported for selecting the extended partitions (Watson et al., 1988; Richmond and Watson, 1990; Nordtvedt et al., 1993). The selection of the extended partition was not explicitly considered here.

Analysis of accuracy

It is important to determine whether the unknown functions can be determined accurately from the data that are to be measured in the displacement experiment. We use a Monte Carlo procedure introduced by Richmond (1988) to evaluate the estimation of the experiment about the estimated parameters (Kerig and Watson, 1986), but includes the linear inequality constraints.

Measurement errors are represented as the difference between the measured data and the corresponding values calculated with the true parameters:

$$\boldsymbol{\epsilon} = \boldsymbol{Y} - \boldsymbol{F}(\boldsymbol{\beta}_t). \quad (12)$$

Each set of measurement errors will result in a corresponding set of errors in the parameter estimates:

$$\delta\boldsymbol{\beta} = \boldsymbol{\beta}_e - \boldsymbol{\beta}_t. \quad (13)$$

The parameter errors that correspond to a specific set of measurement errors are obtained solving the following minimization problem:

$$\min H(\delta\boldsymbol{\beta}) = [\boldsymbol{\epsilon} - A_t \delta\boldsymbol{\beta}]^T \boldsymbol{W} [\boldsymbol{\epsilon} - A_t \delta\boldsymbol{\beta}] \quad (14)$$
$$\text{subject to:} \quad \boldsymbol{G}\delta\boldsymbol{\beta} \geq \boldsymbol{g} - \boldsymbol{G\beta}_t.$$

Pointwise confidence intervals for the estimated flow functions are calculated using a Monte Carlo procedure. A number (say N_{mc}) of realizations of the vector of errors $\boldsymbol{\epsilon}$ is obtained using a pseudorandom number generator. Solving Eq. 14 for each vector of errors generated, N_{mc} sets of parameter errors $\Delta\boldsymbol{\beta}$ are calculated. Then N_{mc} sets of parameter estimates $\boldsymbol{\beta}_e$ are obtained using Eq. 13.

To construct pointwise confidence intervals for the relative permeability and capillary pressure functions, each of the N_{mc} estimated functions were evaluated at a large number of selected sets of saturation values, and the values ordered from

lowest to highest. For example, the ordering for relative permeability i corresponding the saturation values S_I and S_{II} is

$$k_{ri}(S_I,S_{II},\boldsymbol{\beta}_1^{ri}) \le k_{ri}(S_I,S_{II},\boldsymbol{\beta}_2^{ri}) \le \cdots \le k_{ri}\left(S_I,S_{II},\boldsymbol{\beta}_{N_{mc}}^{ri}\right), \tag{15}$$

where $\boldsymbol{\beta}_j^{ri}$ is an estimate of the parameters corresponding to the representation for k_{ri}. The 95% confidence intervals were approximated by discarding the outer 5% of these calculated values. The confidence intervals for the capillary pressure functions were found in a similar fashion.

In this work, subroutines RNSET and RNNOA of the IMSL library (1987) were used to generate pseudorandom numbers with mean zero and variance one. The problem specified in Eq. 14 was solved using subroutine LSEI (Hanson and Haskell, 1982).

Results and Discussion

In this section, the methodology is demonstrated with simulated experimental data that are generated by adding random errors to values calculated with the mathematical model of the experiment. It is important to analyze the estimation problem under these controlled conditions. Since the *true* functions are known, we can test the extent to which we would be able to recover them from a given experimental design.

We show that regions of the functions that are represented by the measured data can be determined accurately using a particular experimental design that could be implemented in the laboratory. This is a significant finding. It indicates that with a suitable experimental design, we should be able to determine three-phase relative permeability and capillary pressure functions. *A priori* assumptions regarding saturation dependence or function shape or elimination of capillary effects are not required.

Simulated experiment

The experimental data were simulated by adding random errors to values calculated using a specified set of conditions and properties in the mathematical model of the experiment, that is,

$$\boldsymbol{Y} = \boldsymbol{F}(\boldsymbol{\beta}_t) + \boldsymbol{\epsilon}. \tag{16}$$

These simulated data were used to estimate the flow functions starting with some initial guess for the parameters. The same conditions and properties were used to generate the confidence intervals.

The simulated three-phase flow experiment is based on a two-phase flow experiment with Berea sandstone studied by Richmond (1988) and Velazquez (1992). Here, we use fluid properties corresponding to water, oil, and gas phases. The two-phase flow functions were used to guide the selection of the three-phase functions. For example, Figure 1 shows the water relative permeability curves corresponding to two mobile phases. We extended the curves to obtain a smooth, reasonable surface for the three-phase water relative permeability function. The other three-phase flow functions were handled in a similar manner. The actual functions specified are discussed further below.

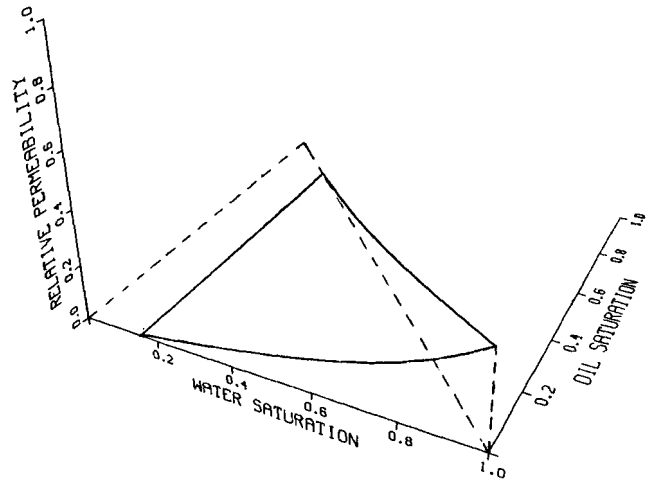

Figure 1. Water relative permeability curves for two mobile phases.

The specified (or *true*) water relative permeability is represented as the tensor product of quadratic B-splines with one knot in each of the S_w and S_o directions. The partition vectors are $y_{S_w}^w = [0.15, 0.15, 0.15, 0.6, 1, 1, 1]^T$ and $y_{S_o}^w = [0, 0, 0, 0.4, 0.85, 0.85, 0.85]^T$, and there are sixteen spline coefficients. Using this representation, $k_{rw} = 0$ at the residual water saturation $S_{wr} = 0.15$. This condition can be seen in the plot of $k_{rw}(S_w, S_o)$ shown in Figure 2. Although this figure shows the k_{rw} function as a surface with positive values in the range $0 \le S_w \le 1$ and $0 \le S_o \le 1$, for simulation purposes, the function is used only for saturation values satisfying the physically necessary condition that $S_w + S_o + S_g = 1$. The intersections of the surface with the planes $S_w + S_o = 1$ and $S_w + S_g = 1$ are the water relative permeability curves corresponding to the water–oil case and the water–gas case, respectively.

The specified oil relative permeability is represented as the tensor product of quadratic B-splines with one interior knot in each direction; $y_{S_w}^o = [0, 0, 0, 0.4, 0.85, 0.85, 0.85]^T$, and $y_{S_w}^o = [0.15, 0.15, 0.15, 0.6, 1, 1, 1]^T$, and there are 16 spline

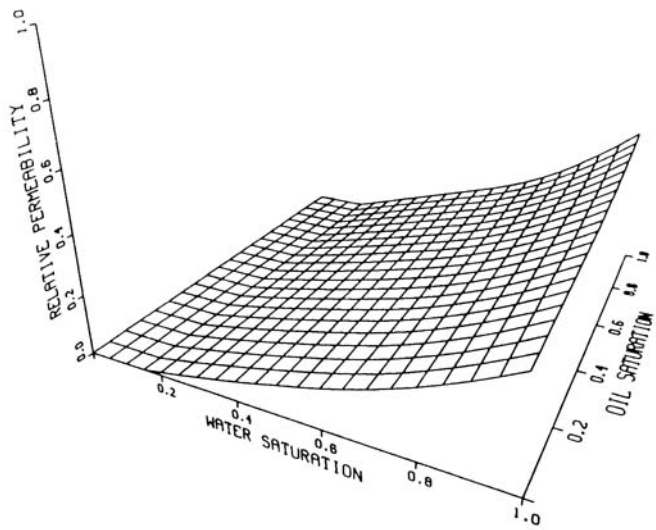

Figure 2. Specified water relative permeability function.

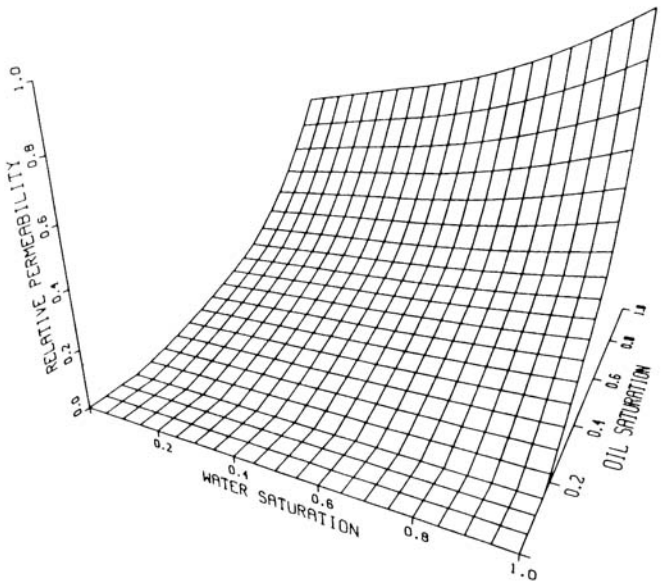

Figure 3. Specified oil relative permeability function.

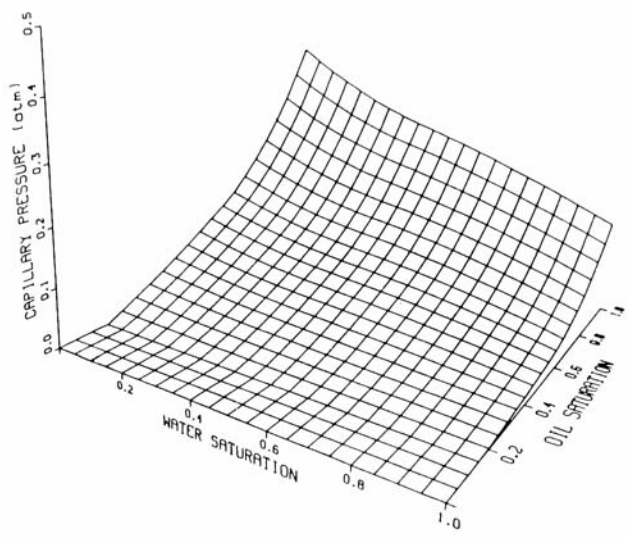

Figure 5. Specified oil–water capillary pressure function.

coefficients. In this representation $k_{ro} = 0$ at the residual oil saturation $S_{ro} = 0.15$. Figure 3 shows a plot of the oil relative permeability function. The intersection of this function with the planes $S_w = 0$ and $S_w + S_o = 1$ are the oil relative permeability curves for the two-phase cases, oil–gas and oil–water, respectively. As for the water permeability, the function is used for only saturation values satisfying $S_w + S_o + S_g = 1$.

Figure 4 shows the specified gas relative permeability function. This is represented as the tensor product of quadratic B-splines with four interior knots in each direction; $y^g_{S_w} = [0, 0, 0, 0, 0.1, 0.25, 0.5, 0.75, 0.9, 0.9, 0.9]^T$ and $y^g_{S_o} = [0, 0, 0, 0, 0.1, 0.25, 0.50, 0.75, 0.9, 0.9, 0.9]^T$, and there are 49 spline coefficients. This function becomes zero for values of $S_g \le S_{gr} = 0.1$, where S_{gr} is the residual gas saturation. For this reason, the coefficients of the B-splines defined for values of saturations greater than $S_w + S_o \ge 1$ are 0. These coefficients need not be estimated in the parameter estimation procedure.

The specified oil–water capillary pressure (P_{cow}) is represented as the tensor product of quadratic B-splines with partitions $y^{cow}_{S_w} = [0, 0, 0, 0.4, 0.85, 0.85, 0.85]^T$ and $y^{cow}_{S_o} = [0.15, 0.15, 0.15, 0.6, 1, 1, 1]^T$, and there are 16 coefficients. A plot of this function is shown in Figure 5. The intersection of the surface with the plane $S_w + S_o = 1$ corresponds to the capillary pressure curve for the oil–water case. As for the oil and water relative permeabilities, this function has positive values in the range $0 \le S_w \le 1$ and $0 \le S_o \le 1$, but for simulation purposes, the function was used only for saturation values satisfying $S_w + S_o + S_g = 1$.

The specified gas–oil capillary pressure (P_{cgo}) is shown in Figure 6. This is represented as the tensor product of quadratic B-splines with partitions $y^{cgo}_{S_w} = [0, 0, 0, 0.15, 0.35, 0.55, 0.7, 0.85, 0.85, 0.85]^T$ and $y^{cgo}_{S_o} = [0, 0, 0, 0.15, 0.3, 0.45, 0.65, 0.85, 0.85, 0.85]^T$, and there are 49 coefficients.

We chose the operating conditions for the simulated experiment to be similar to a case that could actually be per-

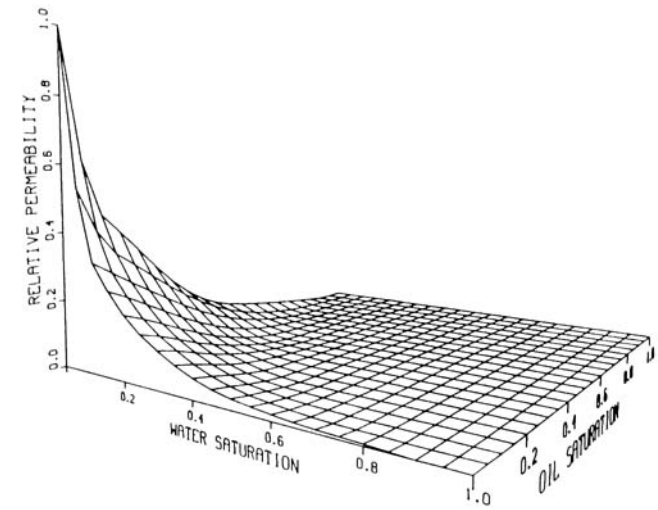

Figure 4. Specified gas relative permeability function.

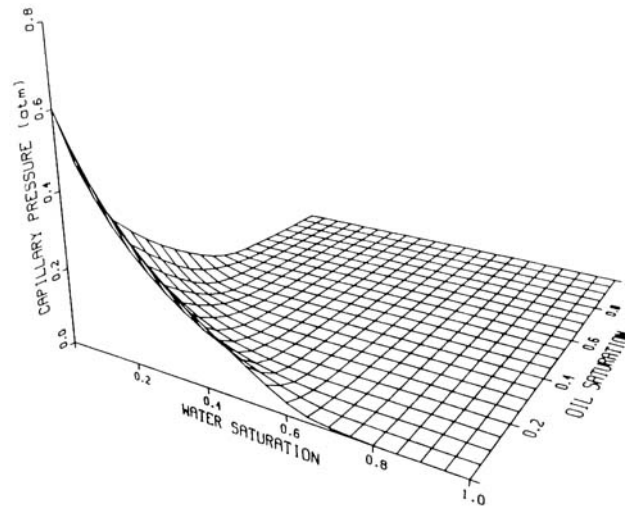

Figure 6. Specified gas–oil capillary pressure function.

Table 1. Properties of the Core Sample and Operating Conditions for the Three-Phase Displacement Experiment

Core properties	k	1,290 md
	ϕ	0.305
	Length	7.62 cm
	Area	5.06 cm^2
	S_{rw}	0.15
	S_{ro}	0.15
	S_{rg}	0
Operating conditions	$\tilde{q}_o$	0.006 cm^3/s
	t_o^i	0 s
	$\tilde{q}_g$	0.006 cm^3/s
	t_g^i	500 s
	μ_w	1.01 cp
	μ_n	3.28 cp
	μ_g	0.01 cp
Total oil and gas injected		0.536 PV

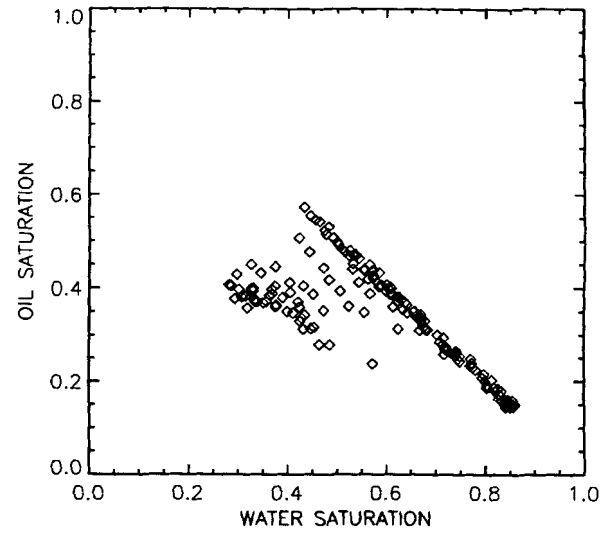

Figure 7. Distribution of saturation data represented in the simulated three-phase displacement experiment.

formed. Using the nomenclature introduced by Saraf et al. (1982), a DDI displacement process is simulated; that is, water saturation is increasing, oil saturation is decreasing, and gas saturation is increasing.

Initially, we take the sample to have been flooded with water to the residual oil saturation. We take oil to be injected, as in a two-phase drainage experiment. At the breakthrough time (around 500 s for this experiment), oil injection is taken to be suspended and the gas phase is injected for another 500 s, just through the breakthrough time of the gas phase. Therefore, the simulated experiment is for 1,000 s. Table 1 shows the properties of the fluid and the core sample, along with the operating conditions for the three-phase displacement experiment.

The simulated data consist of 200 values each of *in situ* water and oil saturation values each 200 values each of *in situ* oil and gas pressures, 100 values each of water and oil production, and 100 values each of oil and gas pressure drop (across the sample). Data were generated uniformly in the range of time $0 \le t \le 1{,}000$ s, that is, the *in situ* data were generated every 5 s and the production and pressure drop data every 10 s. The data were generated by calculating the respective values using the specified multiphase flow functions, and then adding random errors. The random errors were computed by multiplying realizations of a pseudorandom number from a normal distribution with zero mean and unit variance with standard deviations for each of the respective types of measurements. The inverse of the squared standard deviations were used as weights in the minimization of Eq. 9. This corresponds to normalizing the measured data so that the variances of the measured data are unity. Thus, we expect the minimum value of the objective function to be on the order of the total number of experimental data, which is 1,200.

Results of the estimation procedure

This test case was simplified by only estimating those coefficients corresponding to saturation regions for which *in situ* saturation data are available. Of the 146 coefficients, only 45 corresponded to support in the region for which *in situ* saturation data are available (11 of k_{rw}, 11 of k_{ro}, 6 of k_{rg}, 11 of P_{cow}, and 6 of P_{cgo}). The remaining parameters in the *B*-spline representations were kept at the specified values and were not estimated. The saturation values represented by the experimental data are indicated in Figure 7. Note that it is desirable to develop an experimental design that will provide for saturation measurements over a very large region.

The initial guesses for the parameters resulted in an initial value of the objective function of 198,900. The minimum value of the objective functions was obtained after 14 iterations. The value was 1,262. This magnitude is consistent with the value calculated using the specified functions, which was 1,285, and with the number of data (1,200). The estimates of the functions will be discussed in the following subsection. In the remainder of this section, we examine the extent to which the data have been reconciled, and we also discuss some features of the simulated experiment.

In Figures 8–13, plots of the simulated experimental data are shown along with the corresponding values calculated with the estimated functions. The calculated values represent *predictions* of the data, and are identified as such in the figures. Figure 8 shows an excellent match of the simulated water production data. Note that there is deviation from a straight line as the time increases beyond 500 s, corresponding to oil breakthrough in the two-phase drainage part of the experiment. The oil production data, which are also matched well, are shown in Figure 9. This figure also indicates the oil breakthrough time. Significant amounts of oil are produced after the gas is injected.

The oil pressure drop data are plotted in Figure 10. This figure shows the excellent match of the simulated data with the estimated functions. As expected, when a less mobile fluid (oil) displaces a more mobile fluid (water), the pressure drop increases; after the breakthrough time, the saturation of the less mobile fluid increases and its relative permeability is higher; consequently, the pressure drop decreases. The calculated gas-pressure-drop values also show an excellent match of the simulated data, as can be seen in Figure 11. In this figure, the data are plotted for values of $t \ge 500$ s, the time for which the gas phase is injected. The decrease in the gas

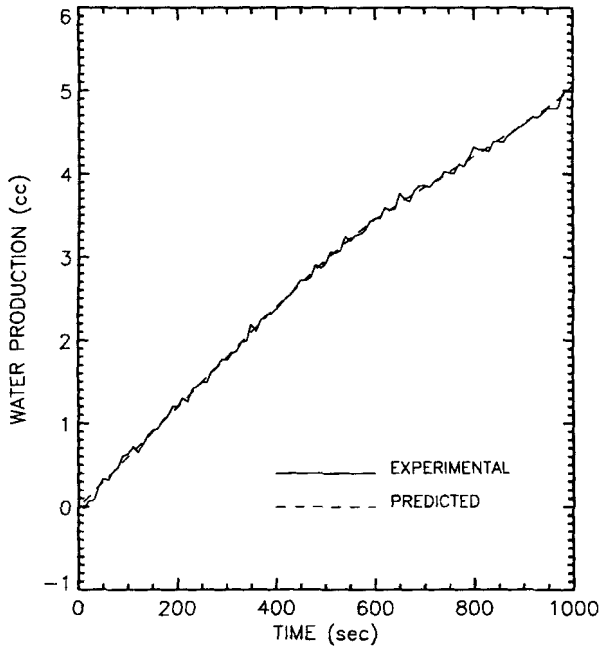

Figure 8. Water production in the simulated three-phase displacement experiment.

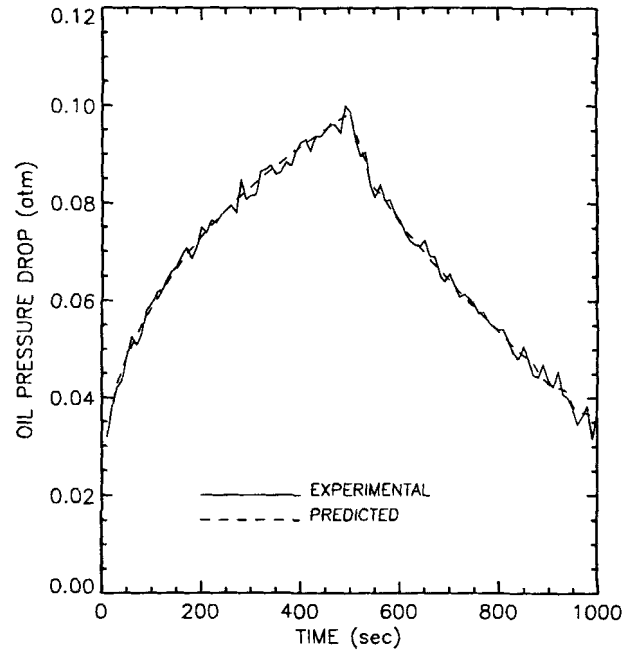

Figure 10. Oil-pressure drop in the simulated three-phase displacement experiment.

pressure drop occurs because the gas phase has a higher permeability than the oil and water phases, and therefore flows at the same rate with lower pressure drop in accordance with Darcy's law.

Figure 12 shows simulated and calculated water saturation profiles corresponding to several times. Each diamond corresponds to a simulated datum; the data corresponding to a specific time are connected with a solid line, and the corresponding values calculated using the estimated functions are connected with a dashed line. The spatial position at which we took *in situ* data to be available were at positions 0.1, 0.2, ..., 0.9. For clarity of presentation, only eight of the twenty-two profiles are shown. The saturation data were well reconciled. The four highest profiles correspond to the time for which oil is injected ($t \leq 500$ s). The remaining four profiles correspond to the time for which gas is injected ($500 \leq t \leq 1{,}000$ s). In the figure, we can also observe the capillary end effect. This effect occurs since the water is taken to be the wetting phase; at the outlet face of the core sample, $P_{cow} = 0$ at $S_{or} = 0.15$.

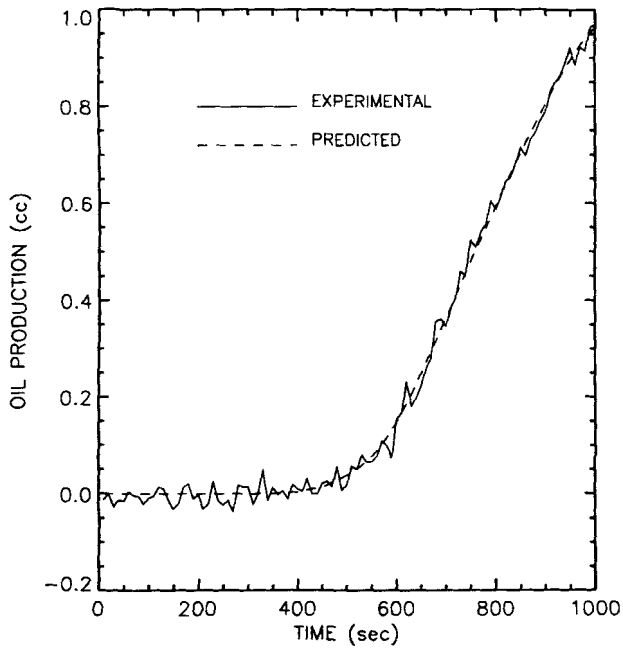

Figure 9. Oil production in the simulated three-phase displacement experiment.

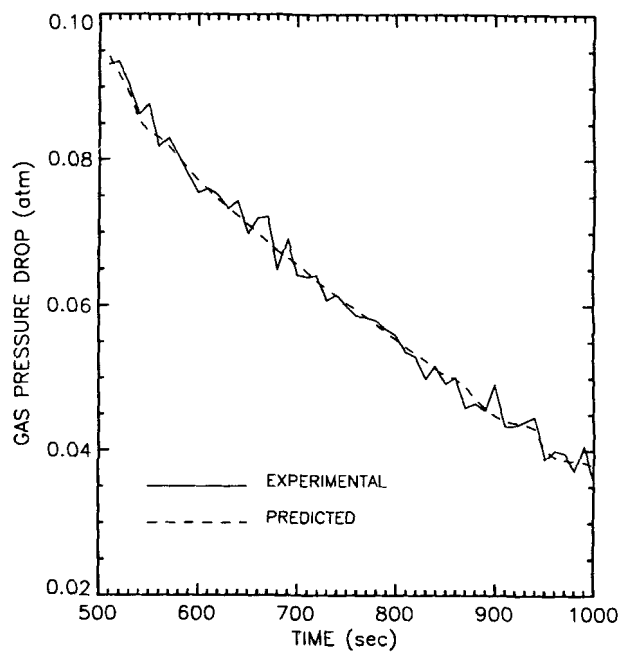

Figure 11. Gas-pressure drop in the simulated three-phase displacement experiment.

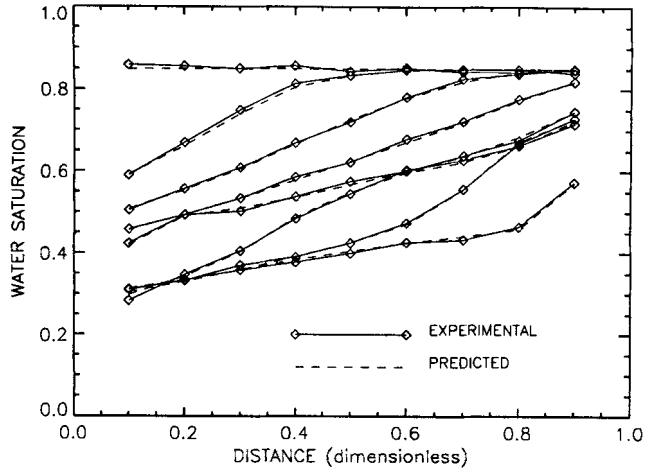

Figure 12. Water-saturation data in the simulated three-phase displacement experiment.

Four oil-saturation profiles are shown in Figure 13 corresponding to the time for which gas is injected ($t \geq 500$ s). These profiles show the depletion of the oil phase by the injected gas. This figure shows that the simulated data are well reconciled by calculations with the estimated properties.

Accuracy of the estimated flow functions

Pointwise confidence intervals were computed for the estimated flow functions using the reported procedures. For each property, two surfaces corresponding to upper and lower confidence intervals can be generated. There are two other surfaces of interest, namely the true and estimated properties. Presentation of multiple surfaces would not be instructive. Instead, we can view these as projections on a plane corresponding to a fixed value of one of the saturations. In the following paragraphs we discuss the accuracy of the estimated oil relative permeability and oil–water capillary pressure in the planes $S_g = 0.1$ and $S_g = 0.3$. We obtained similar results for the other relative permeability and capillary pressure functions.

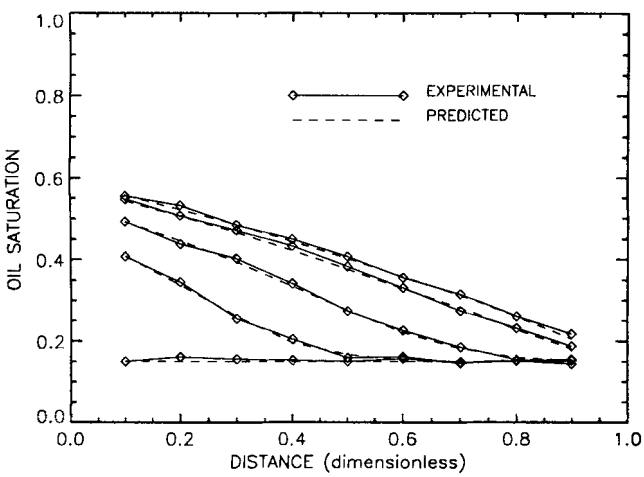

Figure 13. Oil-saturation data in the simulated three-phase displacement experiment for $t \geq 500$ s.

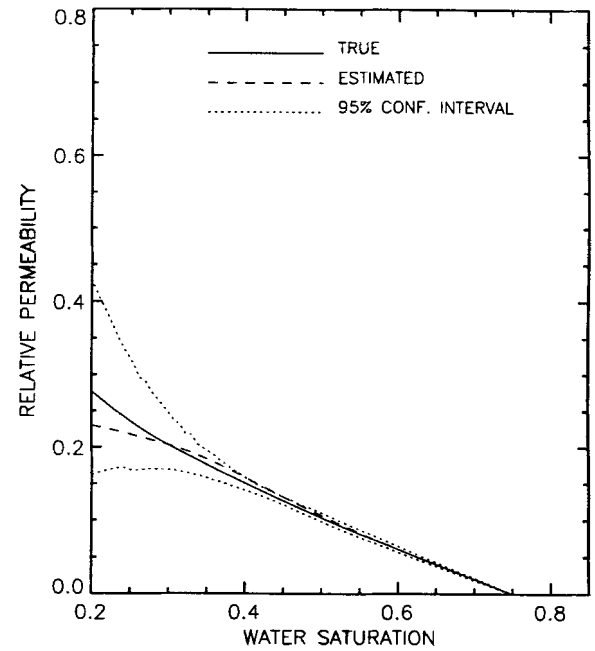

Figure 14. Estimated oil relative permeability and confidence intervals in the plane $S_g = 0.10$.

Figure 14 shows the estimated and true oil relative permeabilities corresponding to $S_g = 0.1$, along with the confidence intervals. This shows that an accurate estimate was obtained. The confidence intervals show that the oil relative permeability can be determined accurately in the range for which *in situ* saturation data are available ($S_w \geq 0.43$). The confidence intervals converge to zero at the value of $S_{or} = 0.15$, where the relative permeability was constrained to be zero.

Figure 15 shows plots of the estimated and true oil relative permeability and its confidence intervals in the plane $S_g = 0.3$.

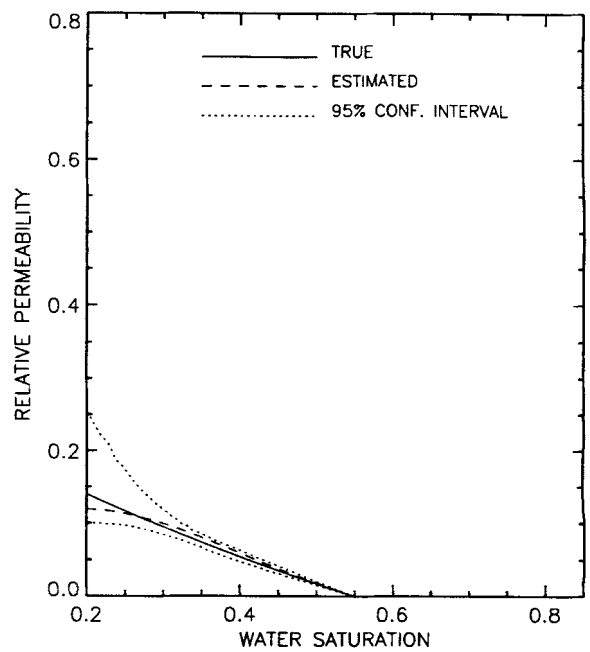

Figure 15. Estimated oil relative permeability and confidence intervals in the plane $S_g = 0.30$.

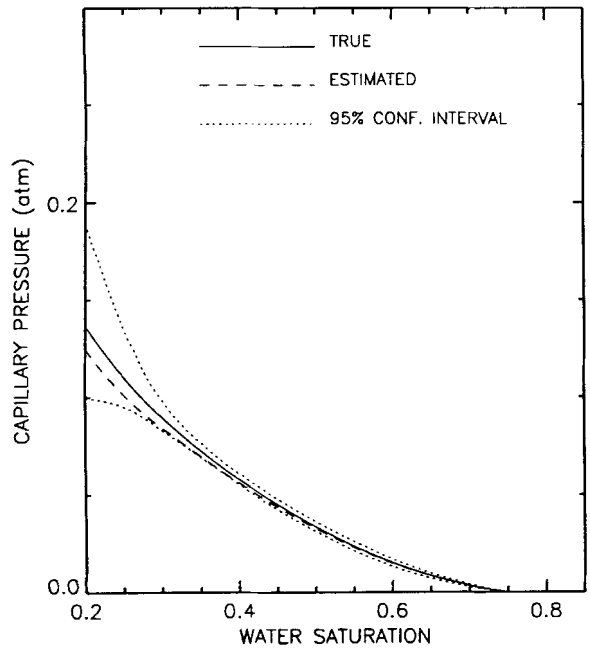

Figure 16. Estimated oil–water capillary pressure and confidence intervals in the plane $S_g = 0.10$.

The results are similar to those for the previous figure. The oil relative permeability can be estimated accurately in the region for which saturation data are available ($S_w \geq 0.28$).

The estimated and true oil–water capillary pressure and confidence intervals corresponding to the value $S_g = 0.1$ are plotted in Figure 16, and those corresponding to the value $S_g = 0.3$ are shown in Figure 17. Both figures show that the capillary pressure function can be estimated accurately in saturation regions for which saturation data are available (i.e., $S_w \geq 0.4$ and $S_w \geq 0.28$, respectively).

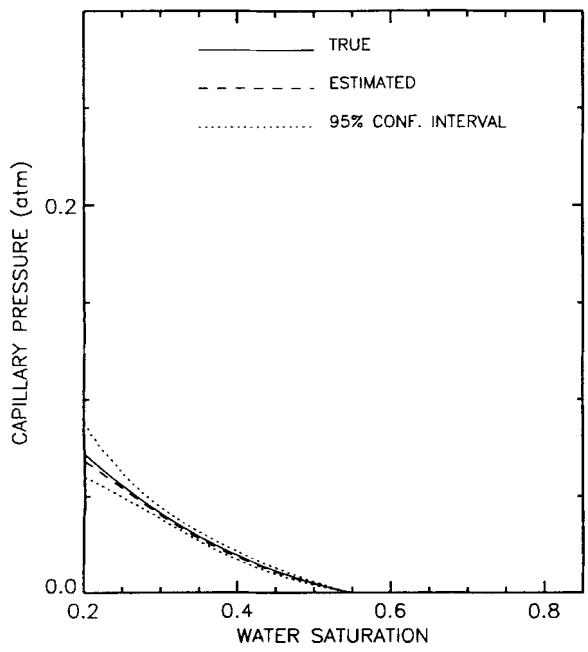

Figure 17. Estimated oil–water capillary pressure and confidence intervals in the plane $S_g = 0.30$.

Conclusions

1. Methodology was presented to estimate simultaneously three-phase relative permeability and capillary pressure functions from displacement experiments. The methodology is quite general and can be used with many different experimental designs or conditions. No special assumptions regarding the saturation dependence or shape of the multiphase flow functions are made.

2. The procedure was demonstrated with simulated experimental data. An analysis of the accuracy of the estimated properties showed that with a suitable experimental design, all the properties can be accurately estimated in saturation regions for which measurements are available.

Acknowledgment

The authors thank the Department of Energy, the Advanced Technology Program of the State of Texas, and the University-Industry Cooperative Research Program for Petrophysical and Reservoir Engineering Applications of NMR for partial support of this research. One of the authors (G.M.M.) also thanks CONACYT in Mexico for providing partial funding for his research stay at Texas A&M University.

Notation

A = sensitivity matrix
$a^i_{k,l}$ = coefficient k,l in tensor–spline representation of relative permeability to phase i
c^{ij}_k = coefficient k of capillary pressure function between phases i and j
$c^{ij}_{k,l}$ = coefficient k,l in tensor–spline representation of capillary pressure between phases i and j
G = matrix of constraints
g = gravity constant
g = righthand side of inequality constraints
g_c = unit conversion constant
H = objective function for the error analysis
J = objective function
k = absolute permeability of core sample
N_{ri} = number of coefficients in relative permeability representation of phase i
N_{cij} = number of coefficients in capillary pressure representation (between phases i and j)
N_{mc} = number of Monte Carlo simulations
$\tilde{q}_i$ = injection rate of phase i, cm/s
q_i = source or sink of phase i, s^{-1}
V_i = formation volume factor of phase i
z = dimension of the core, dimensionless

Greek letters

μ_i = viscosity of phase i, cp
ρ_i = density of phase i, g/cm^3
ϕ = porosity of core sample

Subscripts and superscripts

c = capillary
$c21$ = capillary between phase 2 and 1
$c32$ = capillary between phase 3 and 2
e = estimated
r = relative

Literature Cited

Aleman, M. A., and J. C. Slattery, "Estimation of Three-Phase Relative Permeabilities," *Trans. Porous Media*, **3**, 111 (1988).
Aziz, K., and A. Settari, *Petroleum Reservoir Simulation*, Applied Science, London (1979).

Baker, L. E., "Three-Phase Relative Permeability Correlations," SPE/DOE Symp. Enhanced Oil Recovery, Tulsa, OK (1988).
Bard, Y., *Nonliner Parameter Estimation*, Academic Press, Washington, DC (1974).
Bear, J., *Dynamics of Fluids in Porous Media*, Elsevier, Amsterdam/New York (1972).
Caudle, B. H., R. L. Slobod, and E. R. Brownscombe, "Further Developments in the Laboratory Determination of Relative Permeability," *Trans. AIME*, **192**, 145 (1951).
Corey, A. T., R. J. Rathjens, J. H. Henderson, and M. J. Wyllie, "Three-Phase Relative Permeability," *Trans. AIME*, **207**, 349 (1956).
Corey, A. T., "The Interrelation Between Gas and Oil Relative Permeability," *Prod. Monthly*, No. 1, 38 (1954).
de Boor, C. A., *A Practical Guide to Splines*, Springer-Verlag, New York (1978).
Dietrich, J. K., and P. L. Bondor, "Three-Phase Oil Relative Permeability Models," SPE Fall Technical Conf., New Orleans (1976).
Dria, D. E., G. A. Pope, and K. Sepehrnoori, "Three-Phase Gas/Oil/Brine Relative Permeabilities Measured Under Carbon Dioxide Flooding Conditions," SPE/DOE Symp. Enhanced Oil Recovery, Tulsa, OK (1990).
Dullien, F. A. L., *Porous Media: Fluid Transport and Pore Structure*, 2nd ed., Academic Press, New York (1992).
Fayers, F. J., "Extension of the Stone's Method I and Conditions for Real Characteristics in Three Phase Flow," *SPE Reservoir Eng.*, **4**, 437 (1989).
Grader, A. S., and D. J. O'Meara, "Dynamic Displacement Measurements of Three-Phase Relative Permeabilities Using Three Immiscible Liquids," Proc. Technical Conf. and Exhibition of the SPE, Houston, TX, p. 325 (1988).
Hanson, R. J., and K. H. Haskell, "Algorithm 587: Two Algorithms for the Linearly Constrained Least Squares Problem," *Trans. Math. Software*, **8**, 323 (1982).
Hassler, G. L., and E. Brunner, "Measurements of Capillary Pressures in Small Cores," *Trans. AIME*, 114 (1945).
The IMSL Library, IMSL Inc., Houston, TX (1987).
Johnson, E. F., D. P. Bossler, and V. O. Naumann, "Calculation of Relative Permeability from Displacement Experiments," *Trans. AIME*, 370 (1958).
Kerig, P. D., and A. T. Watson, "A New Algorithm for Estimating Relative Permeabilities from Displacement Experiments," *SPE Reservoir Eng.*, **2**, 103 (1987).
Kerig, P. D., and A. T. Watson, "Relative Permeability Estimation from Displacement Experiments: An Error Analysis," *SPE Reservoir Eng.*, **1**, 175 (1986).
Leverett, M. C., and W. B. Lewis, "Steady Flow of Gas-Oil-Water Mixtures through Unconsolidated Sands," *Trans. AIME*, **142**, 107 (1941).
Manjnath, A., and M. M. Honarpour, "An Investigation of Three-Phase Relative Permeability," SPE Rocky Mountain Regional Meet., Casper, WY (1984).
Mejia, G. M., K. K. Mohanty, and A. T. Watson, "Use of In Situ Saturation Data in Estimation of Two-Phase Flow Functions in Porous Media," *J. Pet. Sci. Eng.*, **12**, 233 (1995).
Nordtvedt, J. E., and K. Kolltveit, "Capillary Pressure Curves from Centrifuge Data by Use of Spline Functions," *SPE Reservoir Eng.*, **6**, 497 (1991).
Nordtvedt, J. E., G. Mejia, P.-H. Yang, and A. T. Watson, "Estimation of Capillary Pressure and Relative Permeability Functions from Centrifuge Experiment," *SPE Reservoir Eng.*, **8**, 292 (1993).
Nordtvedt, J. E., H. Urkedal, A. T. Watson, E. Ebeltoft, K. Kolltveit, K. Langaas, and I. E. I. Øxnevad, "Estimation of Relative Permeability and Capillary Pressure from Transient and Equilibrium Steady-State Data," *Proc. Int. Symp. of Soc. of Core Analysts*, Stavanger, Norway, p. 197 (1994).
Oak, M. J., "Three-Phase Relative Permeability of Water-Wet Berea," SPE/DOE Symp. on Enhanced Oil Recovery, Tulsa, OK (1990).
Oak, M. J., L. E. Baker, and D. C. Thomas, "Three-Phase Relative Permeability of Berea Sandstone," *J. Pet. Tech.*, 1054 (1990).
Oak, M. J., and R. Ehrlich, "A New X-Ray Absorption Method for Measurement of Three-Phase Relative Permeability," *SPE Reservoir Eng.*, **3**, 199 (1988).
Parmeswar, R., and N. L. Maerefat, "A Comparison of Methods for the Representation of Three-Phase Relative Permeability Data," *Proc. California Regional Meet. of SPE*, Oakland, CA, p. 151 (1986).
Richmond, P. C., "Estimating Multiphase Flow Functions in Porous Media from Dynamic Displacement Experiments," PhD Diss., Texas A&M Univ., College Station (1988).
Richmond, P. C., and A. T. Watson, "Estimation of Multiphase Flow Functions from Displacement Experiments," *SPE Reservoir Eng.*, **5**, 121 (1990).
Robinson, R. L., and J. C. Slattery, "Estimation of Three-Phase Relative Permeabilities," *Trans. Porous Media*, **16**, 263 (1994).
Saraf, D. N., and I. Fatt, "Three-Phase Relative Permeability Measurement Using a Nuclear Magnetic Resonance Technique for Estimating Fluid Saturation," *Soc. Pet. Eng. J.*, 235 (1967).
Saraf, D. N., J. P. Batycky, C. H. Jackson, and D. B. Fisher, "An Experimental Investigation of Three-Phase Flow to Water/Oil/Gas Mixtures through Water-Wet Sandstones," San Francisco (1982).
Sarem, A. M., "Three-Phase Relative Permeability Measurements by Unsteady-State Method," *Soc. Pet. Eng. J.*, 199 (1966).
Schneider, F. N., and W. W. Owens, "Sandstone and Carbonate Two and Three-Phase Relative Permeability Characteristics," *Soc. Pet. Eng. J.*, 75 (1970).
Schumaker, L. L., *Spline Functions: Basic Theory*, Wiley, New York (1981).
Slattery, J. C., *Momentum, Energy, and Mass Transfer in Continua*, Kreiger (1981).
Spronsen, E. V., "Three-Phase Relative Permeability Measurements Using the Centrifuge Method," SPE/DOE Symp. Enhanced Oil Recovery, Tulsa, OK (1982).
Stone, H. L., "Probability Model for Estimating Three-Phase Relative Permeability," *J. Pet. Tech.*, 214 (1970).
Stone, H. L., "Estimation of Three-Phase Relative Permeability and Residual Oil Data," *J. Can. Pet. Tech.*, **12**, 53 (1973).
Tao, T. M., and A. T. Watson, "Accuracy of JBN Estimates of Relative Permeability: 1. Error Analysis," *SPEJ*, **24**, 209 (1984a).
Velazquez, G. M., "A Method for Estimating Three-Phase Flow Functions," PhD Diss., Texas A&M Univ., College Station (1992).
Virnovsky, G. A., "Determination of Relative Permeabilities in a Three-Phase Flow in a Porous Medium," *Izv. Akad. Nauk SSSR, Mekh. Zhidk. Gaza*, No. 5 (1984) (in Russian); *Fluid Dyn.*, Engl. transl. (1985).
Watson, A. T., P. C. Richmond, P. D. Kerig, and T. M. Tao, "A Regression-Based Method for Estimating Relative Permeabilities From Displacement Experiments," *SPE Reservoir Eng.*, **3**, 953 (1988).
Watson, A. T., J. H. Seinfeld, G. R. Gavalas, and P. T. Woo, "History Matching in Two Phase Petroleum Reservoirs," *SPEJ*, **20**, 521 (1980).
Weisberg, S., *Applied Linear Regression*, Wiley, New York (1985).
Yang, P.-H., and A. T. Watson, "A Bayesian Methodology for Estimating Relative Permeability Curves," *SPE Reservoir Eng.*, **6**, 259 (1991).

Manuscript received July 5, 1995, and revision received Nov. 16, 1995.